Transactions of the Royal Society of Edinburgh: Earth Sciences, **95**, 87–98, 2004

The influence of cordierite on melting and mineral-melt equilibria in ultra-high-temperature metamorphism

Simon L. Harley and P. Thompson

ABSTRACT: Experimentally constrained calibrations of the incorporation of H_2O and CO_2 into cordierite as functions of P–T-a_{H_2O}-a_{CO_2} are integrated with KFMASH grids which define mineral-melt equilibria in pelites. This is used to explore the impact of the volatile content and composition of cordierite on anatexis and melt-related processes in high-temperature (HT) and ultra-high-temperature (UHT) metamorphism. The strongly temperature-sensitive H_2O content of cordierite coexisting with dehydration melts (0·4–1·6 wt.%) causes a 10–25% relative decrease in the amount of melt produced from pelites compared with models which treat cordierite as anhydrous.

KFMASH melting grids quantified for a_{H_2O} demonstrate consistency between the measured H_2O contents in cordierite from granulite-migmatite terrains and mineral equilibria. These indicate anatexis with a_{H_2O} in the range 0·26–0·16 at 6–8 kbar and 870–930°C. The pressure-stability of cordierite+garnet with respect to orthopyroxene+sillimanite+quartz in KFMASH is strongly influenced by cordierite H_2O content, which decreases from 1·1 to 0·5 wt.% along the melting reaction $Grt+Crd_H+Kfs=Opx+Sil+Qz+L$. The lower-T invariant point involving biotite (8·8 kbar/900°C) that terminates this reaction has a_{H_2O} of 0·16 ± 0·03, whereas the higher-T terminating invariant point involving osumilite (7·9 kbar/940°C) occurs at a_{H_2O} 0·08 ± 0·02. Osumilite-bearing assemblages in UHT terrains imply a_{H_2O} of <0·08, and at 950–1000°C and 8–9 kbar calculated a_{H_2O} is only 0·04–0·02. Cordierites stable in osumilite-bearing assemblages or with sapphirine+quartz have maximum predicted H_2O contents of ca. 0·2 wt.%, consistent with H_2O measured in cordierites from two sapphirine-bearing UHT samples from the Napier Complex.

The addition of CO_2 to the H_2O-undersaturated (dehydration-melting) system marginally decreases the temperature of melting because of the stabilisation of cordierite, the solid product of the peritectic melting reactions. The preferential incorporation of CO_2 enhances the stability of cordierite, even at fixed a_{H_2O}, and causes the stability fields of Grt+Crd+Sil+Kfs+Qz+L and Grt+Opx+Crd+Kfs+Qz+L to expand to higher pressure, and to both higher and lower temperatures. The minimum solubility of H_2O in granitic melt is independent of the CO_2 content of cordierite, and the distribution of H_2O between melt and cordierite is similar at a given melt H_2O-content to the H_2O-only system. This enhanced stability of CO_2-bearing cordierite leads to a reduced stability range for osumilite-bearing assemblages to temperatures of ca. 950–975°C or greater. Cordierites in the Napier Complex UHT gneisses contain 0·5 and 1·05 wt.% CO_2, consistent with a role for CO_2 in stabilising cordierite with respect to osumilite in these unusual sapphirine-bearing granulites.

KEY WORDS: Fluids, granites. granulites, osumilite, sapphirine.

The H_2O-CO_2-bearing phase cordierite (Schreyer 1985) is involved in many key mineral equilibria in high-temperature (HT) and ultra-high-temperature (UHT) metamorphism (Hensen 1971, 1986; Hensen & Green 1973; Aranovich & Podlesskii 1989; Vry *et al.* 1990; Bertrand *et al.* 1991; Harley 1998a). It is also central to many of the reactions controlling melting (Vielzeuf & Holloway 1988; Patiño Douce & Johnston 1991; Carrington & Harley 1995a; Stevens *et al.* 1995; Holland *et al.* 1996; Harley 1998a; White *et al.* 2001), being a modally and texturally significant phase in regional granulite terranes which exhibit migmatisation, melt mobilisation and melt extraction (Waters 1988; Fitzsimons 1994, 1996; Harley 1994; Harley *et al.* 2002). From the viewpoint of peraluminous granite melt production in the middle crust, dehydration-melting of biotite-bearing mineral assemblages in pelites with moderate to high X_{Mg} (>0·5) is often controlled by divariant, or higher variance, cordierite-forming reactions such as the model KFMASH (K_2O-FeO-MgO-Al_2O_3-SiO_2-H_2O) reaction:

$$\text{Biotite}+\text{Sillimanite}+\text{Quartz}+\text{K-feldspar}=\text{Cordierite}+\text{Liquid} \quad (\text{R1})$$

producing cordierite migmatites and cordierite-bearing leucogranites at 2·5–7 kbar and 750–900°C (e.g. Waters 1988; Fitzsimons 1996; Kriegsman 2001). Hence, an understanding of the consequences of cordierite as a volatile-bearing phase that can take up H_2O and CO_2 is critical to evaluation of melting processes and useful for the calculation of fluid activities potentially accompanying melt production. With respect to HT and UHT metamorphism, the stability of cordierite in both the presence and absence of melt generally defines the lower temperature (T) and pressure (P) limits of mineral assemblages such as sapphirine+quartz and orthopyroxene+sillimanite+quartz, which are critical to establishing the progress and conditions of UHT metamorphism. Therefore, an understanding of the stability limits of cordierite and their dependence on its H_2O and CO_2 content is central to any evaluation of UHT metamorphism and

https://doi.org/10.1017/S0263593300000948

the role of melts and melt extraction in stabilising UHT assemblages (e.g. Harley 1998a; Kriegsman 2001; White & Powell 2002; Kelsey *et al.* 2003).

In the present contribution, the authors first overview and summarise the experimental constraints on the P–T-a_{H_2O}-a_{CO_2} dependencies on the uptake of H_2O and CO_2 in cordierite, and the distribution of H_2O between coexisting granitic melt and cordierite. They then go on to integrate this data with phase equilibrium experiments and calculations pertinent to HT/UHT melting and metamorphism in order to examine the impact of cordierite as a peritectic phase in migmatites, and the effect of CO_2 on melting and other phase relations. Finally, they also document and evaluate fluid activities calculated based on cordierite compositions from selected HT and UHT terrains.

1. Incorporation of H_2O and CO_2 into cordierite under HT/UHT conditions

The importance of cordierite as a phase with variable H_2O and CO_2 has long been recognised (Goldman *et al.* 1977; Newton & Wood 1979; Armbruster & Bloss 1982; Aines & Rossman 1984). This is expressed in its general formula (Mg, Fe)$_2$Al$_4$Si$_5$O$_{18}$.nH$_2$O.mCO$_2$, where ‘n’ and ‘m’ are the number of molecules of H_2O and CO_2 respectively, per nine cations (18 oxygen volatile-free) formula unit. It should be noted that this formula is a simplification of the chemistry of cordierite, which also generally incorporates alkalis (Li, Na, K) and Be in its structure (Goldman *et al.* 1977; Armbruster & Bloss 1982; Schreyer 1985; Kalt, 2000). However, Na and K do not appear to exert a strong influence on the H_2O and CO_2 uptake in cordierite compared with the effects of P–T and fluid composition (Thompson *et al.* 2002). The uptake of H_2O and CO_2 by cordierite under fluid-present conditions has been assessed in several experimental studies which have generally involved equilibrating (or attempting to equilibrate) natural or synthetic cordierite with H_2O, H_2O-CO_2 or CO_2 fluids under P–T conditions in the range 1–9 kbar and 500–800°C (Mirwald *et al.* 1979; Kurepin 1985; Boberski & Schreyer 1990; LeBreton & Schreyer 1993; Carey 1995; Skippen & Gunter 1996).

Using a different approach to these earlier studies, Carrington & Harley (1996), Harley & Carrington (2001) and Thompson *et al.* (2001) equilibrated cordierite with peraluminous haplogranitic melt under both fluid-saturated and -undersaturated conditions, and in fluid-present experiments with pure H_2O and with mixed H_2O-CO_2 fluids. These experiments at P–T conditions of 3, 5 and 7 kbars and 800, 900 and 1000°C have enabled the formulation of new expressions relating the activity of H_2O (Harley & Carrington 2001) and CO_2 (Harley *et al.* 2002) to the volatile contents of cordierite as measured by SIMS, and moreover, have defined the P–T-a_{H_2O} dependence of the distribution of H_2O between melt and cordierite, D_w (Harley & Carrington 2001). As with many of the earlier studies, and despite the spectroscopic evidence for distinct orientations for H_2O in the cordierite channels (Armbruster & Bloss 1982; Schreyer 1985; Winkler *et al.* 1994), these experiments have demonstrated that a simple, one-site model adequately describes the incorporation of both H_2O and CO_2 in P–T-a_{H_2O}-a_{CO_2} space. This one-site model defines the maximum total number of molecules of H_2O (n) and CO_2 (m) potentially incorporated into cordierite to be unity (i.e. n+m=1).

In the case of the incorporation of H_2O into cordierite, the saturation H_2O contents determined by Harley & Carrington (2001) are consistent with the majority of the previous lower-T experimental data in the cordierite-H_2O system (Mirwald *et al.* 1979; Boberski & Schreyer 1990; Mukhopadhyay & Holdaway 1994; Carey 1995; Skippen & Gunter 1996). Hence, Harley & Carrington (2001) combined their data with the previous work to obtain a P–T-a_{H_2O} relationship for cordierite that is applicable over the T range 600–1000°C:

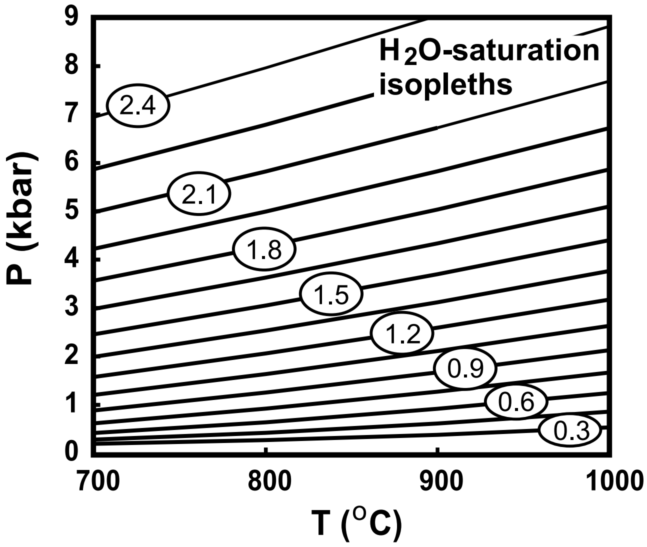

Figure 1 Pressure–temperature diagram contoured with isopleths (isohydrons) of H_2O in $X_{Mg}=0{\cdot}75$ cordierite coexisting with pure H_2O fluid, as modelled by Harley & Carrington (2001). The isohydrons are expressed in terms of wt.% H_2O.

$$a_{H_2O}=[n/(1–n)].(\exp\{[-4203(\pm 320)/T]+11{\cdot}75(\pm 0{\cdot}33)\})/f_{H_2O(P,T)} \quad (1)$$

Setting $a_{H_2O}=1$ and solving for ‘n’ at specified P,T and f_{H_2O}(P,T) produces the H_2O isopleths (also known as isohydrons) presented in Figure 1. These isohydrons are within the error range of isopleths calculated from the thermodynamic data set of Holland & Powell (1998).

Of significance for melting relationships in HT and UHT metamorphism, the wt.% H_2O incorporated into melt and cordierite at specified P–T in H_2O-undersaturated conditions (i.e. Crd+L) and up to H_2O fluid saturation (i.e. Crd+L+V) are systematically correlated (Harley & Carrington 2001; Harley *et al.* 2002). When considered in terms of a_{H_2O}, a linear relationship exists between n/(1–n) in cordierite and the a_{H_2O} functions which describe H_2O uptake in melt as based on the Burnham model (Burnham 1994; Holloway & Blank 1994), but fitted using the H_2O solubility data of Holtz & Johannes (1994) and Johannes & Holtz (1996). This relationship allows modelling of the variation in D_w, the distribution of H_2O between peraluminous granitic melt and cordierite as a function of P–T and a_{H_2O}. D_w is defined as:

$$D_w=[\text{wt.\% } H_2O(\text{melt})]/[\text{wt.\% } H_2O(\text{Crd})] \quad (2)$$

The H_2O distribution curves presented in Figure 2 are calculated from the models developed by Harley & Carrington (2001) based on their experimental data. At low melt H_2O contents in the range 1–3·5 wt.% (those likely to be typical of HT/UHT melts), D_w values are generally in the range 2·5–5·0. As considered in Harley *et al.* (2002) and below, such D_w values impact on the amount of melt that can be produced in a cordierite-forming dehydration-melting reaction compared with dehydration-melting reactions in which cordierite does not participate.

The incorporation of CO_2 into cordierite and its modelling has been the subject of several investigations based on cordierite-fluid exchange experiments (e.g. Johannes & Schreyer 1981; Kurepin 1985; Le Breton & Schreyer 1993). The

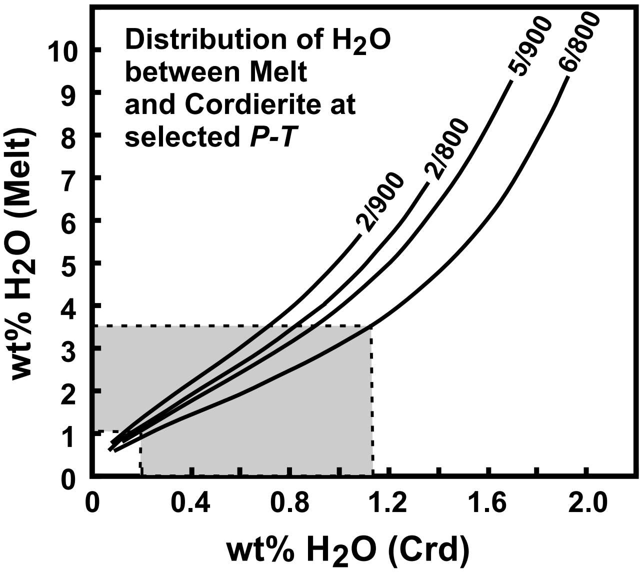

Figure 2 Modelled distribution curves of H_2O between cordierite and coexisting granitic melt, calculated from the a–X relationships for cordierite and melt presented by Harley & Carrington (2001), for selected high-temperature P–T conditions (e.g. 2/900 is 2 kbar and 900°C). Note that D_w at a selected P–T condition and cordierite H_2O content can be calculated from this diagram simply by dividing the appropriate wt.% H_2O (melt) by wt.% H_2O (Crd). The shaded field depicts the H_2O contents typical of cordierite coexisting with high-temperature/ultra-high-temperature melts.

exchange experiments have internal inconsistencies and appear to fail to achieve equilibrium (Le Breton & Schreyer 1993), rendering previous modelling tenuous. However, Thompson *et al.* (2001) and Harley *et al.* (2002) have recently reported and summarised the results of cordierite-granitic melt experiments conducted in the presence of mixed H_2O-CO_2 fluids. Extrapolation of the linear relationships which exist between a_{CO_2} and m/(1–m) in these experiments allows calculation of the maximum quantity of CO_2 that can be taken up by cordierite at unit a_{CO_2} for each P, T condition. The P–T- a_{CO_2} dependence of the incorporation of CO_2 into cordierite P–T range 3–7 kbar and 800–1000°C is then described by the following equation:

$$a_{CO_2}=[m/(1–m)].(\exp\{[-3073(\pm200)+(0{\cdot}3023P)]/T+13{\cdot}1(\pm1{\cdot}2)\})/f_{CO_2(P,T)} \quad (3)$$

Setting $a_{CO_2}=1$ and solving for 'm' at specified P–T and f_{CO_2}(P,T) produces CO_2 isopleths like those presented in Figure 3. Equation 3 and the calculated isopleths, which are consistent with one of the experimental cordierites used by Johannes & Schreyer (1981), are used here in the consideration of the effects of CO_2 on HT/UHT equilibria involving cordierite.

As an independent check on the validity of the cordierite-granitic melt experiments conducted in the presence of mixed H_2O-CO_2 fluids, the H_2O contents of melt and CO_2-bearing cordierite have been measured (Thompson *et al.* 2001). The D_w calculated from these data (e.g. for a given P–T condition and melt H_2O content) are consistent with those modelled from the H_2O-undersaturated experiments of Harley & Carrington (2001). This indicates ideal or near-ideal behaviour of H_2O and CO_2 in the channel site of cordierite, and furthermore, implies that CO_2 has negligible impact on distribution of H_2O between melt and cordierite, at least at temperatures of 800°C and above. In other words, the H_2O contents of H_2O-CO_2-bearing cordierite can be used to deduce the H_2O contents of any fugitive melts formerly coexisting with cordierite under HT/UHT conditions. This applies so long as the HT/UHT melts are close to the experimental leocogranitic melts in terms of their major element chemistries, such as Na/K and SiO_2 contents (Thompson *et al.* 2002), or can be corrected to account for differences in these parameters. In the present work, the experimental cordierite-melt data will be applied to analyse mineral-melt reaction systematics in KFMASH. This involves correction of the melt H_2O model to account for the lack of Na. In practice, this correction is very small (<0·5 wt.% H_2O in melt at saturation: Holtz & Johannes 1994; Johannes & Holtz 1996), and within the error range of the experimental data and model (<0·1 wt.% H_2O in melt) for the range of low-a_{H_2O} conditions considered in the analysis presented herein.

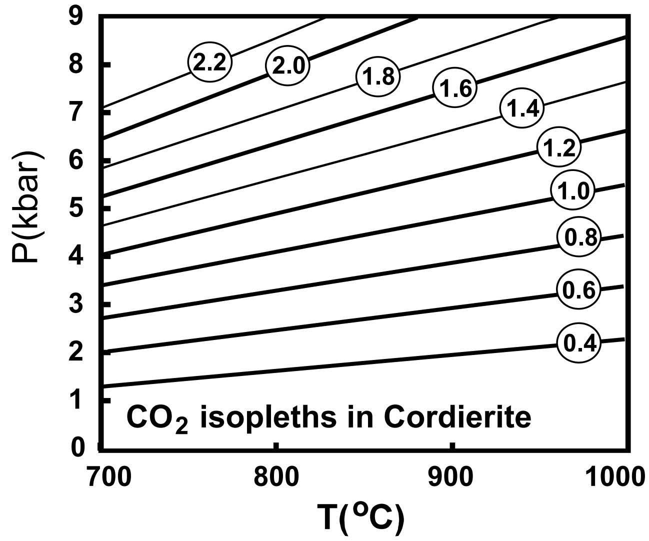

Figure 3 Pressure–temperature diagram contoured with the isopleths of CO_2 in X_{Mg}=0·80 cordierite coexisting with pure CO_2 fluid, as modelled by Thompson *et al.* (2001) and Harley *et al.* (2002). The isopleths are expressed in terms of wt.% CO_2.

Equations 1 and 3 allow calculation of the saturation values (molecules p.f.u. or wt.%) of both H_2O and CO_2 in cordierite at any intermediate H_2O-CO_2 fluid composition providing an appropriate fluid *a*-X relation is used for H_2O-CO_2 mixing. In the present study, as in previous work (Thompson *et al.* 2001; Harley *et al.* 2002), the authors have adopted the same fluid H_2O-CO_2 *a*-X model as applied to the experiments, i.e. the CORK model of Holland & Powell (1990). The saturation H_2O-CO_2 channel fluid contents and channel X_{CO_2} attainable in cordierite coexisting with peraluminous granitic melts produced through 'dehydration' melting in the presence of a low-a_{H_2O}, CO_2-rich fluid phase will be investigated and tested in comparison with natural rocks, following an analysis of the impact of cordierite volatile contents on melting and phase relations in HT/UHT model systems.

2. Impact of cordierite on percentage melting: H_2O distribution systematics

As noted in the introduction and demonstrated in the seminal work of Waters (1988), dehydration-melting of biotite-bearing mineral assemblages in magnesian pelites (X_{Mg} >0·5) is often controlled by cordierite-forming reactions such as the KFMASH divariant equilibrium:

$$\mathrm{Bt+Sil+Qz+Kfs=Crd+L} \quad \text{(R1)},$$

which is related to the KFMASH univariant reaction:

$$\mathrm{Bt+Sil+Qz+Kfs=Grt+Crd+L} \quad \text{(R2)}$$

(Fig. 5a). Reaction R2 is also recognised as a multivariant equilibrium controlling melting in more complex natural rock systems and case studies (e.g. Fitzsimons 1996; White *et al.* 2001).

Consideration of cordierite as a H_2O-bearing phase shows that its formation as a peritectic phase via reaction R1 decreases the volume percentage of melt produced from the dehydration-melting of biotite-bearing pelites. This was first recognised by Harley (1994), who defined the distribution of H_2O between melt and cordierite (now denoted as D_w=wt.% H_2O_{melt}/wt.% H_2O_{crd}), and suggested, on the basis of one reconnaissance experiment, that this distribution coefficient was 3·3 ± 0·5. Stevens *et al.* (1995) indirectly produced D_w values (2·1 ± 0·3 to 1·5 ± 1·1 at 800–1000 °C) for a series of melting experiments at 5 kbar using modal mass-balance calculations, and suggested that the proportion of melt produced would be 'severely' restricted. Direct experimental determination of cordierite and melt H_2O contents (Carrington & Harley 1996; Harley & Carrington 2001) demonstrated that dehydration-melts coexist with cordierites which contain 0·4–1·6 wt.% H_2O, depending on P–T. Modelling of D_w as a function of P,T and a_{H_2O} shows that D_w lies in the range 2·5–5·0 for dehydration melting in the P–T field 5–9 kbar and 850–1000 °C (e.g. Fig. 2). Based on mass-balance calculations in KFMASH, D_w values of this magnitude cause a 15–30% relative decrease in the amount of melt produced from reaction R1 compared with the analoguous reaction assuming anhydrous cordierite or with melting reactions involving garnet, which may operate at similar P–T conditions, but in Fe-richer bulk compositions. An example of this behaviour is illustrated in Figure 4, which shows the impact of cordierite wt.% H_2O on the relative amount of melt produced when that melt contains 2 wt.% H_2O, corresponding to temperatures of 900–950 °C at 5–8 kbar. In this case, the amount of melt is reduced by some 20%. The general conclusion from this is that the amount of melt produced from slightly more magnesian, cordierite-bearing pelites will be less than that produced from garnet-bearing pelite at the same P–T conditions – the cordierite-bearing lithologies will appear more refractory.

Using the same logic, for a specific bulk rock composition, the amount of melt produced at lower-P where cordierite is stable in preference to garnet in a pelite with intermediate X_{Mg} (=0·40–0·60) will be some 20% (relative) less than that predicted from analyses which ignore the impact of cordierite H_2O on the stoichiometry of the melting reactions. Moreover, since K-feldspar is consumed in proportion to the amount of melt produced (Fig. 4), some 50% (relative) less K-feldspar is consumed in the cordierite-bearing case. Hence, K-feldspar will persist to higher temperatures if it initially is present in similar modal amounts in Mg- and Fe-pelites. These considerations also apply to all calculations of pseudosections involving cordierite at HT/UHT conditions (e.g. White *et al.* 2001; Kelsey *et al.* 2003). Decreased melt production means that K-feldspar will persist to higher-T, and hence, be able to participate in osumilite-forming reactions; for example, in bulk compositions which otherwise may be modelled to lose K-feldspar, and hence, not intersect potential osumilite-producing reactions, such as those depicted in Figure 5a. Hence, consideration of cordierite as a phase that sequesters H_2O in the melting regime extends the range of KFMASH bulk compositions (in terms of A'KF) which are accessible to osumilite. Pseudosections which attempt to illustrate the mineral assemblages stable with melt in specific pelite rock compositions in HT/UHT metamorphism must recognise and incorporate the effect of H_2O in cordierite on the percentage melt production and residual solid phase assemblage if they are to be realistic and informative.

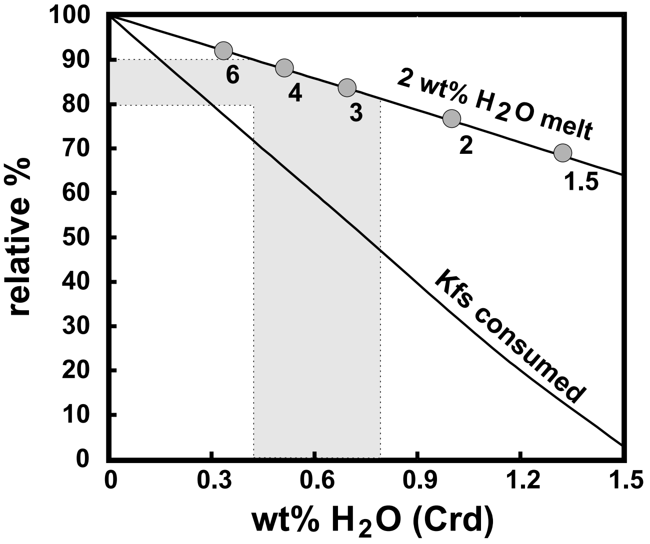

Figure 4 Relative proportion of melt produced and K-feldspar consumed (normalised to 1 for the case of anhydrous cordeierite) in a model pelite initially containing 25% biotite for the case in which the P–T conditions of melting result in a melt with 2 wt.% H_2O (e.g. 5·5 kbar/900 °C to 9·5 kbar/950 °C; see Fig. 5a). The relative proportions of melt produced and K-feldspar consumed in the reaction (R1) decrease as the H_2O-content of coexisting cordierite increases and D_w (numbers below filled circles) decreases [i.e. as P increases along the 2 wt.% H_2O (melt) isopleth in Fig. 5a]. The shaded field depicts the H_2O contents typical of cordierite in this case, which lead to a decrease in melt production to 80–90% of the amounts expected if the H_2O content of cordierite is ignored.

3. Integration of cordierite-melt H_2O data with UHT reaction grids: predicted cordierite H_2O contents and a_{H_2O} conditions in HT/UHT metamorphism

The H_2O contents of cordierite coexisting with melt, and the a_{H_2O} conditions along KFMASH dehydration-melting reactions involved in HT/UHT metamorphism (Carrington & Harley 1995a; Harley 1998a; White *et al.* 2001; Kelsey *et al.* 2003), can be calculated based on knowledge of the variation in the minimum H_2O content of peraluminous granitic melt with P, T and D_w over the same P–T domain (Harley & Carrington 2001). Contours of minimum melt H_2O contents (Holtz & Johannes 1994; Johannes & Holtz 1996) are superimposed on the KFMASH petrogenetic grid involving the phases Grt, Crd, Bt, Sil, Opx, Qz, Kfs, L and Os developed by Carrington & Harley (1995a, b) and modified in the light of calculations by subsequent workers (Holland *et al.* 1996; White *et al.* 2001; Kelsey *et al.* 2003) in Figure 5a. Using the D_w relationships implicit in Figure 2 and described in Harley & Carrington (2001), this grid also has been contoured for the H_2O content of cordierite coexisting with these dehydration-melts. Like the melt H_2O content isopleths, but in contrast to cordierite H_2O saturation isohydrons, the cordierite H_2O isopleths relevant to dehydration melting are strongly temperature-dependent, varying from 1·2 to 1·4 wt.% H_2O at 800 °C to less than 0·2 wt.% H_2O at 1000 °C. Moreover, comparison of these isopleths with the assemblage fields defined by the KFMASH grid shows that cordierites coexisting with dehydration melts in the assemblage Bt+Sil+Crd+Qz+Kfs+L should generally contain >1·2 wt.% H_2O (melt H_2O >3 wt.%), whereas cordierites in the higher-T migmatite

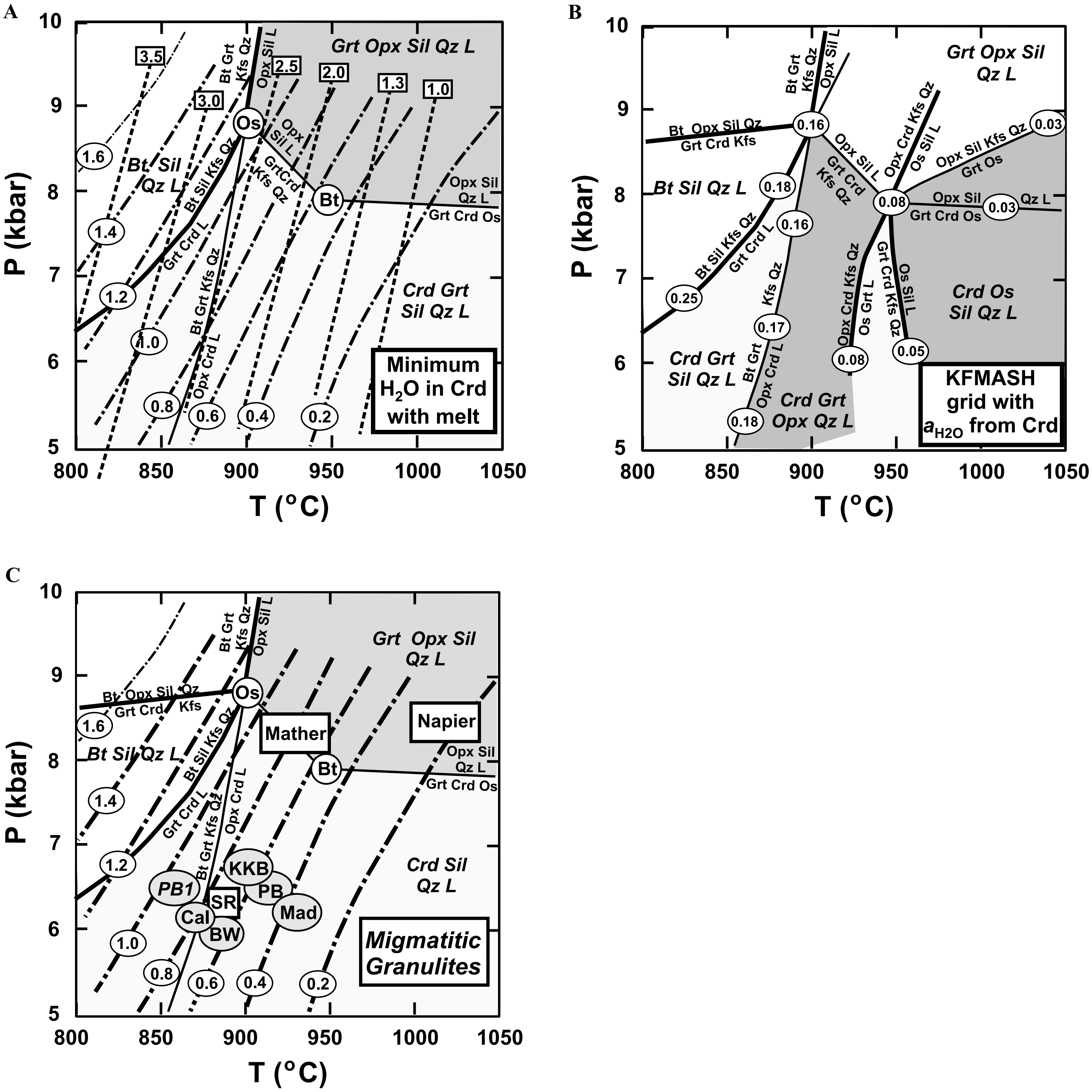

Figure 5 (A) Contoured pressure–temperature (P–T) diagram depicting cordierite-melt H_2O relationships for conditions where the melt has its minimum possible H_2O content at P and T. Contours of minimum melt wt.% H_2O (dashed lines annotated with wt.% H_2O values in rectangles) are after Johannes & Holtz (1996) and Harley & Carrington (2001). Contours of cordierite wt.% H_2O (dot-dashed lines annotated with wt.% H_2O values in ellipses) are derived from the D_w-a_{H_2O} relationships defined in Harley & Carrington (2001) and calculated using Equation 1 for a_{H_2O} compatible with those defined by the melt isopleths. The heavy solid lines are KFMASH system reactions which limit the stabilities of key cordierite-bearing assemblages (e.g. Crd+Grt+Sil+Qz+L) These reactions are based on Carrington & Harley (1995a), as modified by White *et al.* (2001), and are focused on the osumilite-absent, [Os], and biotite-absent, [Bt], invariant points (see Fig. 5b for other related KFMASH equilibria). (B) A P–T diagram depicting KFMASH system reactions based on Carrington & Harley (1995a, b), as modified by White *et al.* (2001), and focused on the osumilite-absent, [Os], and biotite-absent, [Bt], invariant points of Fig. 5a. These invariant points have associated a_{H_2O} values of 0·16 and 0·08 respectively (see text for discussion). Selected KFMASH reactions are labelled at specific P–T conditions for a_{H_2O} calculated from the modelled cordierite H_2O contents (Harley & Carrington 2001; see Fig. 5a). Selected mineral assemblage fields are illustrated by shading. (C) A P–T diagram as in Figure 5a, contoured for the H_2O contents of cordierite formed in equilibrium with KFMASH granitic melt, illustrating the P–T conditions of equilibration of the Crd+Sil migmatites (ellipses) and Crd+Opx migmatites/granulites (rectangles) listed in Table 1. The P–T conditions inferred from independent equilibria are in reasonable agreement with measured cordierite H_2O contents in most cases (Mad: Madagascar; KKB: Kerala Khondalite Belt; Cal: Calabria; BW: Bayerische Wald; SR: Strangways Range; Mather; Napier), but peak temperature estimates for Prydz Bay (*PB1*) are significantly lower than would be deduced from cordierite in this case (PB). Sources for P–T estimates are given in Table 1 along with the relevant cordierite compositional data.

assemblage Grt+Crd+Sil+Qz+Kfs+L should preserve H_2O contents in the range 1·1–0·2 wt.%, depending on T. Cordierite in the assemblage Crd+Opx+Qz+Kfs+L, which lies to higher-T than the KFMASH univariant:

$$\mathrm{Bt+Grt+Kfs+Qz=Opx+Crd+L} \qquad \mathrm{(R3)}$$

is constrained to contain <0·8 wt.% H_2O for all UHT P–T conditions apart from those near the [Os] invariant point at 8·8 kbar and ca. 900 °C.

The volatile content of cordierite formed through dehydration-melting is critical to the stability of cordierite+garnet with respect to assemblages such as orthopyroxene+sillimanite+quartz and sapphirine+quartz (Aranovich & Podlesskki 1989; Bertrand *et al.* 1991; Carrington 1995; Carrington & Harley 1995a; Holland *et al.* 1996; Aranovich & Berman 1996). As shown in Figure 5a, a pronounced change in melt H_2O contents in the 900–950 °C interval coupled with an increase in D_w from 2·4 to 3·0 leads to a marked decrease in cordierite H_2O from 1·1 to 0·5 wt.% along the univariant reaction that joins the two invariant points equivalent to [Os] and [Bt] in the grid of Carrington & Harley (1995a), and limits the stability of Fe-Mg garnet+cordierite in this system:

$$\mathrm{Grt+Crd_H+Kfs=Opx+Sil+Qz+L} \qquad \mathrm{(R4)}$$

where Crd_H denotes hydrous cordierite in equilibrium with the dehydration melt. The negative dP/dT slope of this reaction is consistent with and, at least in part, reflects this marked decrease in channel occupancy. Cordierite that persists with Opx+Sil+L at pressures above those of reaction R4 is predicted to contain 1·1–0·4 wt.% H_2O over the temperature range 900–970 °C. It is also clear from Figure 5a that cordierite coexisting with osumilite can only contain up to 0·5 wt.% H_2O and would generally contain less (<0·4 wt.%) in UHT terrains.

Using Equation 1, a_{H_2O} along the dehydration-melting reactions and at the invariant points in the KFMASH grid (Carrington & Harley 1995a; Holland *et al.* 1996) has been calculated (Fig. 5b). These a_{H_2O} values vary from 0·24 at 6·7 kbar and 825 °C to 0·16 at 8·8 kbar and 900 °C in the case of Reaction R2, and from 0·18 at 5 kbar to 0·16 at 8·8 kbar along the very steep (dP/dT=85 bar/°C) Reaction R3. The a_{H_2O} values calculated for the two key KFMASH invariant points using the present authors' cordierite and melt models are 0·16 ± 0·03 at the lower-T [Os] point (8·8 kbar/900 °C), and only 0·08 ± 0·02 at the [Bt] point (7·9 kbar/940 °C) where the osumilite+garnet assemblage becomes stable and overlaps with assemblages involving orthopyroxene+sillimanite+quartz+melt (Carrington & Harley 1995b). From this, we can infer that the osumilite-bearing assemblages equilibrated at 7–9 kbar in the Napier Complex of East Antarctica (Ellis *et al.* 1980; Grew 1982; Audibert *et al.* 1995) and other UHT terrains imply a_{H_2O} of <0·08.

The contoured KFMASH melting grids (Fig. 5a, b) are consistent with independent P–T estimates obtained from garnet+cordierite+sillimanite migmatitic granulites from the Kerala Khondalite Belt (Nandakumar & Harley 2000), southern Madagascar (Markl *et al.* 2000) and Calabria (Schenk 1984). SIMS H_2O measurements on cordierites from these terrains yield a_{H_2O} conditions in the range 0·06–0·18 (Table 1) and imply cordierite-melt equilibrium at P–T conditions in the range ca. 6–7 kbar and 860–930 °C, depending on terrain (Fig. 5c). The H_2O contents of former melts which equilibrated with these low-H_2O (0·6–1·2 wt.%) cordierites are 1·3–2·2 wt.%. Based on measured cordierite CO_2 contents, calculated a_{CO_2} in these migmatitic granulites are high (0·34–0·85) but consistent with fluid-undersaturation in all examples except Calabria. This is considered further in section 5 below.

The H_2O contents of cordierites from cordierite-sillimanite migmatites from the Bayerische Wald have been determined by informed spectroscopy (IR) techniques by Kalt (2000). The average H_2O content of cordierite based on all the measured samples in this case is 0·53 ± 0·10 wt.%, although one sample preserves cordierite with up to 0·74 wt.% H_2O. This most hydrous cordierite is consistent with equilibrium with granitic melt containing 2·5 wt.% H_2O at the upper end of the P–T conditions preferred by Kalt (2000) for the metamorphic peak in this region based on geothermobarometric calculations (BW, Fig. 5c.: ca. 6 kbar, 870 °C). The majority of samples which preserve lower H_2O contents could be interpreted to indicate melt loss at higher temperatures (up to 900 °C), but could equally reflect post-peak loss or leakage of H_2O from the cordierite channels in this case.

A similar interpretation could be put forward for cordierites in the garnet+cordierite+sillimanite migmatitic granulites of Prydz Bay, East Antarctica (Fitzsimons 1994, 1996). The H_2O contents, measured by SIMS, of these cordierites are only 0·35–0·60 wt.% and average at ca. 0·5 wt.% (Table 1; Harley *et al.* 2002). Such low H_2O contents would be consistent with cordierite-melt equilibrium at 6·5 kbar and 900–930 °C (PB, Fig. 5c), whereas geothermometry corrected for the effects of Fe-Mg exchange and phase equilibrium considerations indicate peak temperatures of 860 °C (Fitzsimons 1996). If the latter temperatures are accepted (*PB1*, Fig. 5c) then the cordierite that coexisted with melt according to Figure 5c would have contained >0·8 wt.% H_2O, implying that all of the cordierites measured from the Prydz Bay granulites have lost between 25% and 50% of their initial H_2O. Such marked H_2O loss is not required to explain the volatile contents and phase relations of most of the other examples considered here and in Harley *et al.* (2002), particularly in the cases where the cordierites contain significant CO_2 (e.g. BB4: 0·6 wt.% CO_2). Hence, although the present authors cannot discount the possibility that some H_2O leakage has occurred from cordierite, they suggest that the peak temperatures attained in the Prydz Bay granulites were higher than those deduced by Fitzsimons (1996) and in the range 900–930 °C.

Also depicted in Figure 5c are the preferred P–T conditions for three examples of cordierite-orthopyroxene HT/UHT granulites. Migmatitic garnet+orthopyroxene+cordierite granulite from Strangways Range (Arunta Complex) and garnet+orthopyroxene+cordierite ± sillimanite granulite from Mather Peninsula (Harley 1998b) both lie on the 0·7 wt.% H_2O isopleth and indicate temperatures wholly consistent with independent estimates from geothermobarometry. At UHT conditions of greater than 1000 °C at 8–9 kbar, as recorded from several localities in the Napier Complex of East Antarctica (Ellis *et al.* 1980; Sheraton *et al.* 1987; Harley & Hensen 1990; Harley & Motoyoshi 2000), a_{H_2O} values calculated using cordierite-melt equilibria (Fig. 5b; Table 1) are only 0·04–0·02. Any cordierite stable in osumilite-bearing assemblages, or with sapphirine+quartz in the presence of melt, would be expected to have H_2O contents of only 0·2 wt.%; lower H_2O cordierites would be present if melting did not occur. Two samples from the Napier Complex preserve cordierites containing 0·2 wt.% H_2O (Table 1), consistent with this expectation (Fig. 5c).

4. Melting and migmatisation in the H_2O-CO_2 system

So far, the present authors have considered only the impact of cordierite as a H_2O-bearing phase involved in melting and

Table 1 Volatiles in cordierites from selected high-temperature and ultra-high-temperature granulites/migmatites*

Sample	Cordierite							P (kbar)	T (°C)	a_{H_2O}	a_{CO_2}	Melt	
	X_{Mg} (Crd)	H_2O (wt.%)	CO_2 (wt.%)	n (pfu)	m (pfu)	m+n (pfu)	X_{CO_2}					H_2O wt.%)	D_w
Bayerische Wald (Kalt 2000)													
BW-44ii	0·60	0·740	0·051	0·255	0·007	0·262	0·027	6·0	900	0·178	0·033	2·5	3·3
BW-average	0·60	0·528	0·064	0·180	0·009	0·189	0·048	6·0	900	0·115	0·041	1·8	3·5
Crd-Sil migmatite		*0·095*	*0·018*	*0·032*	*0·003*	*0·032*	*0·013*			*0·025*	*0·012*	*0·3*	
Prydz Bay migmatitic granulites, Antarctica (Fitzsimons 1994, 1996)													
BB4 (17)	0·66	0·494	0·583	0·168	0·081	0·250	0·325	6·0	860	0·096	0·361	1·7	3·5
Grt-Crd-Sil migmatite		*0·090*	*0·118*	*0·031*	*0·016*	*0·038*	*0·045*			*0·028*	*0·122*	*0·4*	
Calabria, Serre Massif (Schenk 1984)													
8–90 (170)	0·63	0·805	1·305	0·272	0·181	0·453	0·400	6·5	875	0·162	0·853	2·2	2·7
Grt-Crd-Sil migmatite		*0·060*	*0·060*	*0·021*	*0·008*	*0·027*	*0·014*			*0·014*	*0·041*	*0·4*	
Kerala Khondalite Belt, Southern India (Nandakumar & Harley 2000)													
SHED10 (10)	0·60	0·636	0·854	0·219	0·120	0·340	0·355	6·5	900	0·129	0·557	2·0	3·1
Grt-Crd leucosome		*0·036*	*0·022*	*0·012*	*0·006*	*0·010*	*0·011*			*0·013*	*0·019*	*0·3*	
Chittikara-SLH (12)	0·60	0·633	0·762	0·218	0·108	0·326	0·330	6·5	900	0·128	0·490	2·0	3·1
Grt-Crd leucosome		*0·112*	*0·053*	*0·039*	*0·012*	*0·020*	*0·043*			*0·030*	*0·043*	*0·6*	
SE Madagascar (Markl *et al.* 2000)													
patch migmatite (8)	0·86	0·287	0·527	0·095	0·072	0·167	0·431	6·0	920	0·057	0·344	1·3	4·5
Crd leucosome		*0·050*	*0·065*	*0·017*	*0·009*	*0·022*	*0·029*			*0·016*	*0·074*	*0·3*	
Strangways Range, Arunta Complex													
9052 (5)	0·87	0·690	0·023	0·229	0·003	0·232	0·014	6·0	875	0·147	0·013	2·3	3·3
Grt-Opx-Crd patch		*0·092*	*0·005*	*0·031*	*0·001*	*0·031*	*0·004*			*0·030*	*0·004*	*0·3*	
Mather Peninsula, Rauer Islands (Harley 1998b)													
SH/88/218 (8)	0·88	0·698	0·055	0·233	0·008	0·241	0·031	8·5	920	0·091	0·021	1·8	2·6
Grt-Opx-Crd-Sil		*0·067*	*0·021*	*0·022*	*0·003*	*0·024*	*0·008*			*0·009*	*0·011*	*0·3*	
Napier Complex, Enderby Land (Harley, 1986; Sheraton *et al.* 1987)													
49752 Mt Sones (8)	0·88	0·194	0·498	0·064	0·068	0·132	0·513	8·5	1000	0·025	0·256	0·85	4·4
Grt-Spr-Sil-Crd		*0·021*	*0·026*	*0·007*	*0·004*	*0·010*	*0·018*			*0·008*	*0·024*	*0·1*	
49354 Mt Hardy (6)	0·90	0·215	1·040	0·072	0·142	0·214	0·664	8·5	1000	0·028	0·576	0·96	4·3
Spr-Qz-Crd		*0·031*	*0·021*	*0·010*	*0·003*	*0·013*	*0·026*			*0·011*	*0·025*	*0·1*	

(number) number of SIMS volatile analyses of cordierite in the sample. The *P*–*T* estimates used in the calculation of fluid activities are taken from the references given for each case study. Figures given in italics are the 1σ uncertainties in the quoted parameters, propagated from 1σ uncertainties in the analytical populations and SIMS calibrations, and uncertainties in the cordierite activity calibrations of Equations 4 and 8, together with ± 0·5 kbar and ± 30°C uncertainties in the *P*–*T* estimates used in calculation of fluid activities.

mineral reactions in HT/UHT metamorphism and anatexis. However, cordierite also incorporates CO_2 into its channels, and as noted by Thompson *et al.* (2001), the distribution of CO_2 between melt and cordierite is strongly in favour of cordierite, such that $D_C < 0{\cdot}2$ and probably $<0{\cdot}1$. The stability of cordierite as a H_2O-CO_2-bearing phase coexisting with melt and preferentially fractionating CO_2 has important consequences for the character of fluid-melt-rock interactions since the melt segregates, migrates and crystallises in granulite host rocks. This can be demonstrated by consideration of the crystallisation of two initially slightly fluid-undersaturated leucogranitic melts (e.g. 2 wt.% H_2O, 1000 ppm CO_2 at 5 kbar/900°C) which differ only in their X_{Mg} [i.e. Mg/(Mg+Fe)]. Cooling of the Fe-richer melt (e.g. X_{Mg}=0·25) will result in the crystallisation of garnet along with quartz and feldspars at these pressures, continuously enriching the remaining melt in both H_2O and CO_2 until saturation is reached and a CO_2-rich fluid phase is generated. This fluid may be trapped as CO_2-rich but post-peak fluid inclusions in garnet, as seen in some migmatites (e.g. Santosh 1987), or it may react with reduced minerals to precipitate graphite as crystallisation proceeds (e.g. Fitzsimons & Mattey 1995). In contrast, crystallisation of a Mg-richer melt (e.g. X_{Mg}=0·35) to form cordierite plus quartz and feldspars will result in a slower increase in melt H_2O (dependent on D_w) and a decrease in ppm CO_2 in the melt – the latter effect caused by the sequestering of CO_2 by cordierite (at least 5000 ppm CO_2 cf. 500–1000 ppm in the melt). The cordierite-bearing melt or leucosome is unlikely to attain fluid saturation unless external fluids are introduced or rapid decompression occurs, whereby both melt and cordierite exceed their saturation isopleths. In a closed system (i.e. melt batch crystallising in isolation) or in a system in which melt is continously in communication with cordierite, it is likely that all the available CO_2 will be taken up in the cordierite, inhihiting the formation of fluid inclusions, and indeed, of graphite, since fluid–present conditions are not attained. Conversely, if fluid inclusions (Santosh *et al.* 1993) or leucosome-hosted graphite (Fitzsimons & Mattey 1995) are observed in cordierite-bearing migmatites, it is almost certain that externally derived fluid has been introduced into the system. In principle, such fluid-present conditions should be recorded by the volatile abundances in the cordierite and the a_{H_2O} and a_{CO_2} values calculated using Equations 1 and 2. In short, it is significantly more difficult to saturate a cordierite-bearing migmatite terrain than a garnet-dominated migmatite area which lacks cordierite; for similar P–T conditions and percentage melting, higher fluid fluxes are required in the cordierite migmatite case.

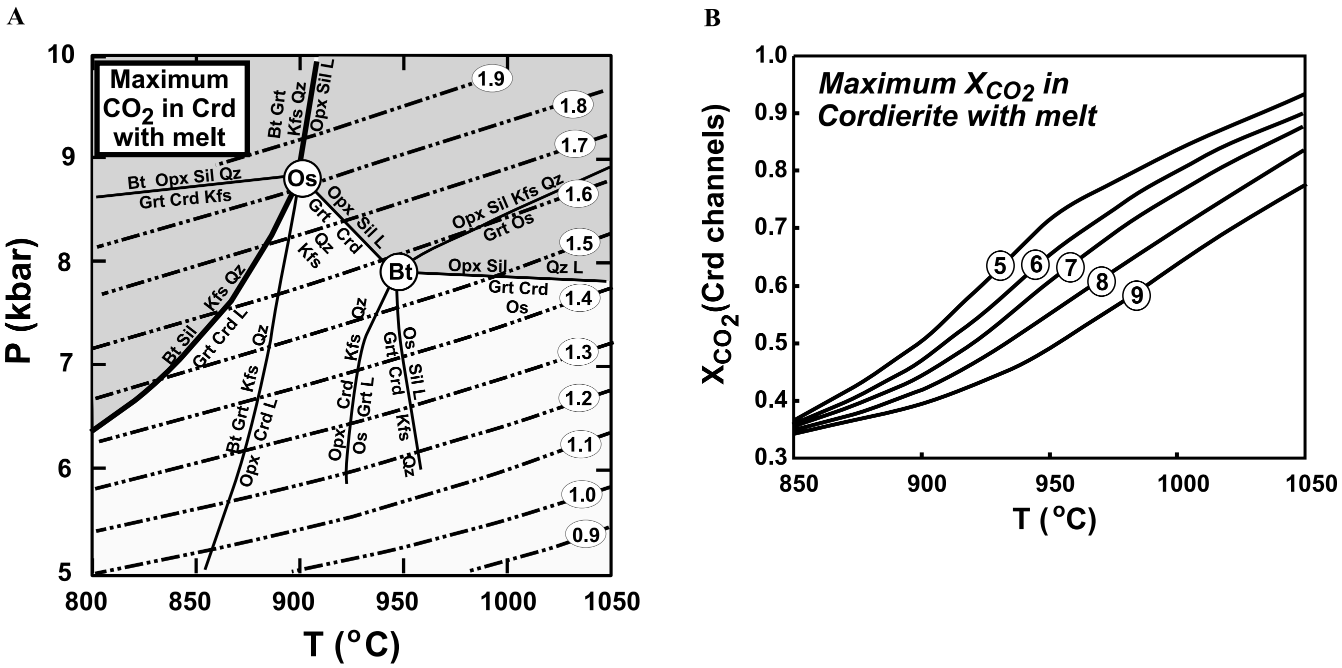

Figure 6 (A) Pressure–temperature (P–T) diagram showing isopleths of the *maximum* CO_2 contents (in wt.%) in cordierite coexisting with melts with minimum H_2O contents (i.e. melts with H_2O contents drawn in Fig. 5a). These isopleths are calculated using Equation 3 (based on Harley *et al.* 2002) in combination with Equation 1. Note that, since cordierite also cotains H_2O, which varies mainly with temperature (Fig. 5a), these CO_2 isopleths do not correspond to those presented for the pure CO_2 system in Figure 3. (B) The *maximum* X_{CO_2} composition of cordierite coexisting with melt and a free-CO_2-dominated fluid phase, plotted as a function of temperature in the melting range for various pressures (in kilobars; denoted by numbers in circles). Corderite coexisting with a low-H_2O melt at 950°C and 7 kbar may contain up to 1·4 wt.% CO_2 (Fig. 6a) and have a channel X_{CO_2} of up to 0·6 without fluid saturation being attained.

5. The effect of CO_2 in cordierite on KFMASH equilibria in HT/UHT metapelites

The contoured grid presented in Figure 5a only includes H_2O dissolved in melt and incorporated in cordierite. If CO_2 is added to this system, it is favourably incorporated into cordierite compared with melt, as noted above, and all other solid phases in the absence of graphite. Given that only a_{H_2O} is fixed, at fixed P–T, by the dehydration melting reactions of Figure 5a, it is possible for cordierites with near-constant H_2O contents but a range of CO_2 contents to be in equilibrium with melts with near-minimum H_2O contents in the KFMASH-CO_2 system. The upper limit on the CO_2 content of cordierite coexisting with melt is that calculated for fluid saturation, but cordierites with low H_2O contents and elevated CO_2 contents which are still less than those required for saturation could coexist with melt alone under fluid-absent conditions.

The maximum (saturation) CO_2 contents of cordierite coexisting with melts formed through biotite dehydration melting are presented as wt.% CO_2 contours in Figure 6a. These isopleths are steeper than and differ from those presented in Figure 3 since they are calculated for fluid saturation in the H_2O-CO_2 system in which a_{H_2O}, and hence, cordierite H_2O content is defined by Crd+L equilibrium. Hence, at lower temperatures, where both cordierite and melt have higher H_2O contents (Fig. 5a), the maximum CO_2 contents attainable in the melt environment are significantly less than those defined for the CO_2-only system of Figure 3, whereas, under HT/UHT conditions, the Crd-L-V isopleths approach those in the CO_2-only system. This is further illustrated by the cordierite channel H_2O-CO_2 composition diagram of Figure 6b, which shows that cordierites with channel X_{CO_2} of up to 0·4 may coexist with melt at 900°C, whilst, at 1000°C, the cordierite channel X_{CO_2} can be as high as 0·6–0·7. The presence of CO_2-rich, high-X_{CO_2} cordierite does not automatically imply the presence of a free carbonic fluid phase in UHT metamorphism or in HT migmatites (Vry *et al.* 1990; Fitzsimons 1994; Harley 1994).

If CO_2 is added to the KFMASH system without the addition of a separate new phase, its favourable incorporation into cordierite will enhance the stability of the mineral, even at fixed a_{H_2O}, and cause all other KFMASH univariant reactions to slide along loci which coincide with the cordierite-absent reactions emanating from the KFMASH invariant points (Carrington 1995). For the H_2O-CO_2 system, Thompson *et al.* (2001, 2002) and Harley *et al.* (2002) have shown that the minimum solubility of H_2O in granitic melt is essentially independent of the CO_2 content of the system and that D_w (Crd-L) is similar at a given melt H_2O content to the H_2O-only system. Hence, the dehydration-melting isopleth sets (Crd and L wt.% H_2O contours) of Figure 5a shift very little with the addition of CO_2 into the cordierite. This behaviour does not apply to saturation H_2O isopleths because, in that case, there is an overall decrease in total volatiles in cordierite at a given P–T as CO_2 enters its channels.

With the addition of CO_2 into cordierite, the KFMASH [Os] and [Bt] points move to higher P and T along (Crd) reactions whereas the H_2O-isopleths remain fixed. Hence, the stability fields of Grt+Crd+Sil+Kfs+Qz+L and Grt+Opx+Crd+Kfs+Qz+L expand to higher pressure, and to both higher and lower temperatures, and KFMASH-C divariant melting fields are generated from the KFMASH univariant dehydration-melting reactions (Fig. 7). Under UHT conditions (>900°C), the high-P stability of Grt+Crd+L, which is bounded up-pressure by the assemblage Opx+Sil+Qz+L, is estimated to be extended by at least 1 kbar on the basis of comparisons between the experimental data of Carrington & Harley (1995a, b) and Bertrand *et al.* (1991), and calculations by Aranovich & Podlesskii (1989). Paradoxically, the addition of CO_2 to the H_2O-undersaturated (dehydration-melting)

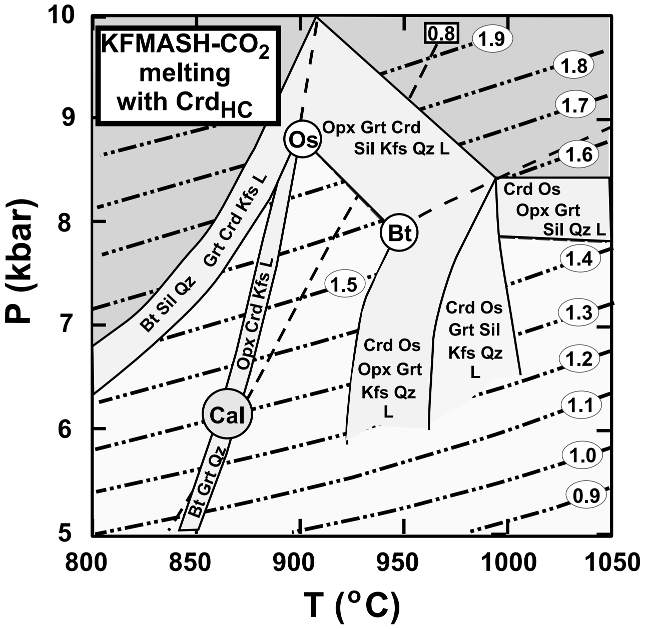

Figure 7 Pressure–temperature (P–T) diagram depicting the offset of selected KFMASH system reactions focused on the [Os] and [Bt] points of Figure 5a as a consequence of the addition of CO_2 to produce the system KFMASH-CO_2. Note that the KFMASH invariant points become lines located along (Crd) equilibria, sliding up-pressure with increasing CO_2 in cordierite. KFMASH univariant reactions become seven phase divariant fields in which cordierite can vary in H_2O and CO_2 depending on P–T (shaded fields). The maximum CO_2 contents of cordierite in these fields are dictated by the isopleths shown (dot-dashed contours in wt.%), which define CO_2 at the offset boundaries of the fields. For example, cordierite in the field Crd+Os+Opx+Grt+Kfs+Qz+L will contain 1·4 wt.% CO_2 at 7·3 kbar, 960°C. Also shown on this diagram is the preferred P–T estimate for the Calabrian cordierite, Cal, which contains 0·8 wt.% H_2O and 1·3 wt.% CO_2 (Table 1). This cordierite lies on the saturation CO_2 isopleth, and hence, suggests equilibration in the presence of melt plus CO_2-rich fluid at ca. 6 kbar and 860°C.

system decreases the temperature of melting, as controlled by the melting reactions which emanate down-pressure from the [Os] point, i.e. melting via equilibria such as R2 and R1 proceeds at lower temperatures in the fluid-saturated and -undersaturated H_2O-CO_2 systems compared with the H_2O-only one, not as a result of CO_2 entering the melt, but rather, reflecting the stabilisation of cordierite, the solid product of the peritectic melting reactions. By stabilising cordierite, it is possible for divariant melting in the presence of a CO_2-rich fluid to progress at temperatures some 20–40°C lower than those required for melting via the reactions noted above (Fig. 7), provided enough H_2O is available to ensure the melt does not crystallise. In other words, the a_{H_2O} must be at least as high as that value defined by the dehydration-melting reaction at the proscribed P–T condition.

The movement of the KFMASH invariant points to higher P also have consequences for the range of volatile compositions attainable by cordierite coexisting with melt. The displaced [Os] point will occur at higher a_{H_2O} and as a result, the cordierite and melt will both have higher H_2O contents (ca. 1·2 and 3 wt.%, respectively) at the saturation condition where CO_2 is in excess but in equilibrium with both Crd and L (10 kbar, 910°C in Fig. 7). The [Bt] point displaces to higher P and T, and therefore, will involve cordierite and melt with marginally lower H_2O contents (0·2 and 1 wt.%, respectively), but the cordierite will have high CO_2 (1·6 wt.%; Fig. 7). As a consequence of these displacements, the high-P limiting reaction involving H_2O-CO_2 cordierite (Crd_{HC}):

$$Grt+Crd_{HC}+Kfs+Qz=Opx+Sil+L \qquad (R4a)$$

occurs at higher pressures and over a broader T range (900–1000°C) in the CO_2-bearing system compared with the KFMASH case, and at ca. 10–9 kbar (Fig. 7). At saturation (high CO_2, low a_{H_2O}, melt still present), this reaction may have a flat to moderately negative dP/dT, dictated by the change in H_2O-CO_2 partitioning between Crd and V across this T range. In the absence of relevant partitioning data, this reaction is drawn parallel to R4 in Figure 7.

6. Consequences for the stability of osumilite in melt-bearing UHT rocks

The uptake of CO_2 by cordierite and its consequent stabilisation to higher P relative to Opx+Sil+Qz has implications for the stability of osumilite and Os+Grt assemblages which may be developed in appropriate KFMASH bulk rock compositions (high-Mg, aluminous) along with melt under UHT conditions (Audibert *et al.* 1995; Carrington & Harley 1995b; Holland *et al.* 1996; White *et al.* 2001). The P–T stability field occupied by osumilite in KFMASH is limited by reactions focused on the [Bt] invariant point (Fig. 5a). Translation of this point up-pressure by a minimum of 0·5 kbar to 8·4 kbar and 990°C, expands the stability field of Grt+Crd +Os+L towards higher pressures. However, the stability fields of Os+Sil+L and Os+Grt+L contract to higher T at pressures less than those of the [Bt] point (Fig. 7). The extent of translation estimated from Figure 7 is of the order of 40–50°C as fluid saturation is approached (i.e. Crd_{HC}+L+V). Hence, under conditions where CO_2-rich cordierite is present, melting involving osumilite will only be seen in UHT granulites at >950–975°C. Cordierite in the sapphirine-bearing but osumilite-absent assemblages from Mount Sones and Mount Hardy in the Napier Complex (Table 1) contain 0·5 and 1·05 wt.% CO_2, respectively, suggesting a role for CO_2 in stabilising cordierite with respect to osumilite, which does occur in other sapphirine-bearing Mg-pelites from these localities.

It is possible that the KFMASH [Bt] point, which is more completely denoted as [Bt, Spr] if sapphirine is considered as an additional UHT mineral, is rendered metastable in CO_2-saturated conditions. This will occur if the displaced (Bt) KFMASH-C reaction involving Crd, Grt, Opx, Sil, Os, Qz and L translates up P and T to intersect the group of UHT reactions which involve Spr+Qz at 1040–1050°C (Bertrand *et al.* 1991; Audibert *et al.* 1995; Carrington & Harley 1995b; Harley 1998a). In this case, the (Bt, Crd, L) reaction of Figure 5b:

$$Opx+Sil+Kfs+Qz=Grt+Os \qquad (Bt, Crd, L)$$

is reduced to zero length, and its high-T terminating invariant point [Bt, Crd, L] will be replaced by others, such as [Bt, Sil, L] and [Bt, Grt, L], which involve Spr+Opx+Os+Qz and CO_2-rich (but H_2O-bearing) cordierite. The linking KFMASH-C reaction:

$$Os+Opx+Crd_{HC}=Spr+Qz+Kfs+L \qquad (Bt, Grt, Sil)$$

will limit cordierite stability to high P–T. Therefore, cordierite with volatile contents of H_2O <0·2 wt.% and CO_2 <1·8 wt.% could, in principle, coexist with all the other UHT phases in the absence of melt.

7. Integration with other UHT indicators: Opx–Crd relationships

Cordierite may coexist with orthopyroxene and melt over a wide range of HT/UHT conditions in rocks of appropriate

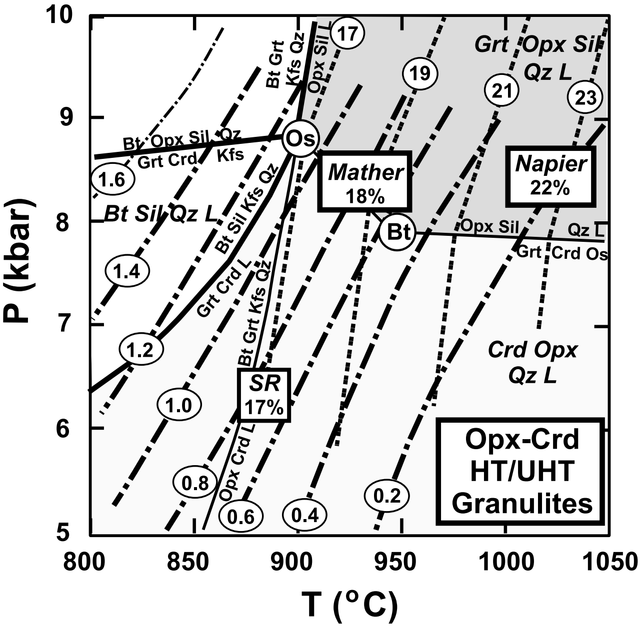

Figure 8 Pressure–temperature (P–T) diagram illustrating the P–T conditions of equilibration of the Crd+Opx migmatites/granulites listed in Table 1. This diagram is contoured for the H_2O contents of cordierite formed in equilibrium with KFMASH granitic melt (dot-dashed lines with wt.% H_2O indicated in ellipses), and for the Al_2O_3 content of orthopyroxene as modelled by Kelsey *et al.* (2003) and expressed in terms of mol% MgTs component. The agreement between the measured cordierite H_2O data and orthopyroxene MgTs contents is good in all three examples. Sources for P–T estimates are given in Table 1 along with the relevant cordierite compositional data; SR: Strangways Range.

bulk composition (Hensen & Green 1973; Carrington & Harley 1995a). At pressures less than those defined by the KFMASH [Os] and [Bt] points (Fig. 5a), relatively magnesian sub-aluminous to moderately aluminous pelites (i.e. compositions below the Grt-Crd tieline on an AFM diagram) may contain Crd+Opx+Qz+L at T>870°C. At higher pressures where the Opx+Sil +Qz+L sub-assemblage is stable, cordierite is restricted in FMAS and KFMASH to highly magnesian bulk compositions lacking garnet (e.g. Hensen 1971; Hensen & Green 1973; Bertrand *et al.* 1991; Carrington & Harley 1995a; Harley 1998a), but may be present along with garnet in slightly less magnesian bulk compositions (X_{Mg} >0·65) if the stabilising effect of CO_2 is considered. When garnet, sillimanite or sapphirine are present along with Opx+Crd, it is possible to estimate the temperatures of metamorphism using the Al_2O_3 content of the orthopyroxene (Ganguly *et al.* 1996; Aranovich & Berman 1997; Harley 1998a, Hollis & Harley 2003; Kelsey *et al.* 2003), and compare such estimates with those inferred from the H_2O contents of the cordierite. This comparison is illustrated for three examples of cordierite-bearing UHT assemblages in Figure 8.

Migmatitic Opx+Sil+Grt+Kfs ± Qz gneisses at Mather Peninsula in the Rauer Islands of East Antarctica have been described in detail by Harley (1998b). These contain magnesian garnet (X_{Mg} >0·66), aluminous orthopyroxene (X_{Mg}=0·78–0·82; Al_2O_3=8·5–10 wt.% zoning up to 12% on rims) and sillimanite in palaeosomes/mesosomes. Similarly, magnesian garnets occur in in 3–10-mm-thick leucosomes along with 2–8-mm-diameter subhedral aluminous orthopyroxene (Al_2O_3=9 wt.%) and microperthite. Locally, the leucosomes also contain cordierite (X_{Mg}=0·90; H_2O= 0·7 wt.%; CO_2=0·06 wt.%), in apparent textural equilibrium with the aluminous orthopyroxene and, by association, with the mesosome assemblage Grt+Opx+Sil. The P–T and a_{H_2O} conditions of extraction and crystallisation of the leucosomes can be assessed from the cordierite H_2O contents by reference to Figure 8. This indicates P–T conditions of ca. 8·5 kbar and 925°C, and a_{H_2O} (Table 1) of 0·09 ± 0·01. In Figure 8, a set of calculated orthopyroxene Al_2O_3 isopleths, expressed in terms of the mol% MgTs (Mg-tschermaks) component, are superimposed on the cordierite H_2O isopleths so that the P–T conditions defined above can be independently assessed. These Al_2O_3 isopleths (Kelsey *et al.* 2003), calculated for the assemblages Grt+Opx+Sil+Qz+L and Grt+Crd+Opx+Qz+L, are in reasonable agreement with those presented by Harley (1998a): over the temperature interval 910°C<T<1050°C, MgTs varies from 17 to 23 mol% in the modelled isopleth set of Kelsey *et al.* (2003), whereas MgTs ranges from 16 to 25 mol% in the Harley (1998a) isopleth diagram. It is encouraging that the MgTs isopleths, cordierite H_2O isopleths and assemblage constraints all match rather well. This suggests that, at least in the present case study, the cordierite has preserved its UHT volatile contents. This is interpreted to reflect melt loss from the Mather Peninsula migmatitic gneiss leucosomes (e.g. Kriegsman 2001; Kelsey *et al.* 2003), which are residual or in their overall chemistry and preserve anhydrous mineral assemblages only partially retrogressed to biotite-bearing ones (Harley 1998b). Melt loss early in the UHT history, and certainly below the peak conditions attained by these rocks (ca. 11–12 kbar, 1030°C; Harley 1998b), is interpreted to have enabled the preservation of the prograde melting record since the leucosomes acted as closed systems following the loss of hydrous melt components.

Grt+Crd+Opx+K-feldspar leucosomes occur as local patchy segregations in semipelitic gneisses near Phlogopite Mine in the Strangways Ranges, which comprise part of the Arunta Complex of central Australia. Cordierite H_2O contents (Table 1) are consistent with dehydration melting via Reaction R3 at 875–900°C if pressures were 6–7 kbar. The orthopyroxene in these leucosome patches contains 7·7 wt.% Al_2O_3, or 17 mol% MgTs, once again consistent with the temperatures implied by the cordierite H_2O data, and therefore, suggestive of melt loss at these conditions, followed by an absence of any fluid that could interact with and hence change the H_2O content of the preserved cordierites.

The final comparison of cordierite H_2O content with the Al_2O_3 contents of orthopyroxene in the same UHT assemblage is provided by the sapphirine+orthopyroxene+quartz granulite from Mount Hardy, East Antarctica (Table 1). This granulite occurs in the UHT sapphirine+quartz zone of the Archaean Napier Complex (Ellis *et al.* 1980; Sheraton *et al.* 1987; Harley & Hensen 1990) and is inferred to have experienced P–T conditions in the region of 8–9 kbar and greater than 1000°C (Harley & Hensen 1990), with even higher temperatures (>1120°C) possible on the basis of comparisons with a sapphirine+orthopyroxene+quartz granulite reported from Mount Riiser-Larsen nearby (Harley & Motoyoshi 2000). Cordierite not only occurs in the Mount Hardy sample as coronas on sapphirine+quartz, but also as large grains in apparent textural equilibrium with orthopyroxene rims which contain up to 10–11 wt.% Al_2O_3, or 22 mol% MgTs. Figure 8 demonstrates that the measured H_2O content of this cordierite (0·22 wt.%) is consistent with the P–T conditions inferred from the orthopyroxene, and is suggestive of the presence of some melt that may have back-reacted with the UHT assemblage to produce this cordierite. Although the CO_2 content of the cordierite is significant (1·04 wt.%), it is not high enough to saturate the cordierite at these P–T conditions, or indeed, any P–T conditions along the post-peak IBC path experienced by the Napier Complex. Hence, in this case, the present authors suggest that the cordierite formed in the absence of a free fluid phase, under low a_{H_2O} (ca. 0·03) and high a_{CO_2} (0·58) conditions mediated by the presence of a small amount of melt.

8. Conclusions

As emphasised in many previous studies (e.g. Hensen 1971; Hensen & Green 1973; Aranovich & Podlesskii 1989; Vry *et al.* 1990; Bertrand *et al.* 1991; Audibert *et al.* 1995; Carrington & Harley 1995a, b; Fitzsimons 1996; Harley 1998a; White *et al.* 2001; Harley *et al.* 2002), cordierite plays a significant role in the high-grade metamorphism and anatexis of pelites. The P–T-dependent H_2O exchange equilibrium between cordierite and granitic melt exerts a strong control on melt production from such rocks. Moreover, the variable CO_2 contents of cordierite formed coexisting with melt influences the P–T positions of melting reactions, expanding the stability fields of cordierite+melt assemblages in KFMASH-CO_2 at the expense of UHT indicator assemblages such as orthopyroxene+sillimanite+K-feldspar+quartz and osumilite+garnet.

SIMS microanalysis of natural cordierites from a selection of HT/UHT migmatitic and granulite terrains yields H_2O contents which are consistent with cordierite-melt equilibrium at temperatures >860 °C, and in most cases, in agreement with calculated KFMASH grids and independent equilibria, irrespective of the CO_2 contents of the cordierites. This gives confidence that volatiles in cordierite, analysed carefully, and with sufficient spatial resolution to evaluate and volatile zoning or leakage, can provide valuable information on the fluid and melting conditions attending HT/UHT metamorphism. With the notable exception of the Calabrian granulites, which appear to have been fluid-saturated at HT conditions and equilibrated in the presence of a CO_2-rich fluid phase at or near peak metamorphic conditions, cordierites from the migmatitic granulites studied thus far yield CO_2 and H_2O contents which produce calculated a_{CO_2} and a_{H_2O} which sum to less than unity. These imply metamorphism under fluid-absent conditions, but in the presence of melts which contain 1·3–2·5 wt.% H_2O and, in many cases, appreciable dissolved CO_2. It is clear that the volatile contents of cordierite in HT/UHT metamorphic and magmatic rocks cannot be assumed to adhere to saturation values or ignored in calculations of mineral and mineral-melt equilibria: they must be routinely measured and incorporated into the assessment and analysis of the P–T and P–T-X-fluid evolution of high-grade terrains.

9. Acknowledgements

This research was supported by NERC grants GR3/9099 and GR3/12573 to S.L.H. We thank John Craven and Richard Hinton (SIMS), and Peter Hill (electron probe) for their assistance with the analysis, Steve Elphick and Damian Carrington for advice on experimental design, and David Mattey, Jim Webster, Volker Schenk and Francois Holtz for their help in producing standards. We are indebted to Bas Hensen, Ian Fitzsimons, Damian Carrington, Ian Buick and Julie Vry for their interest in the cordierite work and discussions of its many implications over the years.

References

Aines, R. D. & Rossman, G. R. 1984. The high-temperature behavior of water and carbon dioxide in cordierite and beryl. *American Mineralogist* **69**, 319–27.

Aranovich, L. Y. & Berman, R. G. 1996. Optimized standard state and solution properties of minerals II. Comparisons, predictions, and applications. *Contributions to Mineralogy and Petrology* **126**, 25–37.

Aranovich, L. Y. & Berman, R. G. 1997. A new garnet-orthopyroxene barometer based on reversed Al_2O_3 solubility in FeO-Al_2O_3-SiO_2 orthopyroxene. *American Mineralogist* **82**, 345–53.

Aranovich, L. Y. & Podlesskii, K. K. 1989. Geothermometry of high-grade metapelites: simultaneously operating reactions. *In* Daly, J. S., Cliff, R. A. & Yardley, B. W. D. (eds) *Evolution of Metamorphic Belts. Geological Society of London, Special Publication* **43**, 45–62. London: Geological Society.

Armbruster, Th. & Bloss, F. D. 1982. Orientation and effects of channel H_2O and CO_2 in cordierite. *American Mineralogist* **67**, 284–91.

Audibert, N., Hensen, B. J. & Bertrand, P. 1995. Experimental study of phase relations involving osumulite in the system K_2O-FeO-MgO-Al_2O_3-SiO_2-H_2O at high pressure and temperature. *Journal of Metamorphic Geology* **13**, 331–44.

Bertrand, P., Ellis, D. J. & Green, D. H. 1991. The stability of sapphirine-quartz and hypersthene-sillimanite-quartz assemblages: an experimental investigation in the system FeO-MgO-Al_2O_3-SiO_2 under H_2O and CO_2. *Contributions to Mineralogy and Petrology* **108** 55–71.

Boberski, C. & Schreyer, W. 1990. Synthesis and water contents of Fe^{2+}-cordierites. *European Journal of Mineralogy* **2**, 565–84.

Burnham, C. W. 1994. Development of the Burnham model for prediction of H_2O solubility in magmas. *In* Carroll, M. R. & Holloway, J. R. (eds) *Volatiles in Magmas. Mineralogical Society of America, Reviews in Mineralogy* **30**, 123–9.

Carey, J. W. 1995. A thermodynamic formulation for hydrous cordierite. *Contributions to Mineralogy and Petrology* **119**, 155–65.

Carrington, D. P. 1995. The relative stability of garnet-cordierite and orthopyroxene-sillimanite-quartz assemblages in metapelitic granulites: experimental data. *European Journal of Mineralogy* **7**, 949–60.

Carrington, D. P. & Harley, S. L. 1995a. Partial melting and phase relations in high-grade metapelites: an experimental petrogenetic grid in the KFMASH system. *Contributions to Mineralogy and Petrology* **120**, 270–91.

Carrington, D. P. & Harley, S. L. 1995b. The stability of osumilite in metapelitic granulites. *Journal of Metamorphic Geology* **13**, 613–25.

Carrington, D. P. & Harley, S. L. 1996. Cordierite as a monitor of fluid and melt water contents in the lower crust: an experimental calibration. *Geology* **24**, 647–50.

Ellis, D. J., Sheraton, J. W., England, R. N. & Dallwitz, W. B. 1980. Osumilite-sapphirine-quartz granulites from Enderby Land, Antarctica – mineral assemblages and reactions. *Contributions to Mineralogy and Petrology* **72**, 123–43.

Fitzsimons, I. C. W. 1994. Cordierite migmatites from East Antarctica: geochemical constraints on volatile distribution during crustal anatexis. *Mineralogical Magazine* **58a**, 274–5.

Fitzsimons, I. C. W. 1996. Metapelitic migmatites from Brattstrand Bluffs, east Antarctica – metamorphism, melting and exhumation of the mid-crust. *Journal of Petrology* **37**, 395–414.

Fitzsimons, I. C. W. & Mattey, D. P. 1995. Carbon isotope constraints on volatile mixing and melt transport in granulite-facies migmatites. *Earth and Planetary Science Letters* **134**, 319–28.

Goldman, D. S., Rossman, G. R. & Dollase, W. A. 1977. Channel constituents in cordierite. *American Mineralogist* **62**, 1144–57.

Ganguly, J., Cheng, W. & Tirone, M. 1996. Thermodynamics of aluminosilicate garnet solid solution: new experimental data, an optimized model, and thermometric applications. *Contributions to Mineralogy and Petrology* **126**, 137–51.

Grew, E. S. 1982. Osumilite in the sapphirine-quartz terrane of Enderby Land, Antarctica: implications for osumilite petrogenesis in the granulite facies. *American Mineralogist* **67**, 762–87.

Harley, S. L. 1986. A sapphirine-cordierite-garnet-sillimanite granulite from Enderby Land, Antarctica: implications for FMAS petrogenetic grids in the granulite facies. *Contributions to Mineralogy and Petrology* **94**, 452–60.

Harley, S. L. 1994. Cordierite as a sensor of fluid and melt distribution in crustal metamorphism. *Mineralogical Magazine* **58a**, 374–5.

Harley, S. L. 1998a. On the occurrence and characterisation of ultra high-temperature (UHT) crustal metamorphism. *In* Treloar, P. J. & O'Brien, P. (eds) *What Controls Metamorphism and Metamorphic Reactions? Geological Society, London, Special Publication* **138**, 75–101. London: Geological Society.

Harley, S. L. 1998b. Ultrahigh temperature granulite metamorphism (1050 °C, 12 kbar) metamorphism and decompression in garnet (Mg70)-orthopyroxene-sillimanite gneisses from the Rauer Group, East Antarctica. *Journal of Metamorphic Geology* **16**, 541–62.

Harley, S. L., Thompson, P., Buick, I. S. & Hensen, B. J. 2002. Cordierite as a sensor of fluid conditions in high-grade metamorphism and crustal anatexis. *Journal of Metamorphic Geology* **20**, 71–86.

Harley, S. L. & Carrington, D. P. 2001. The distribution of H_2O between cordierite and granitic melt: improved calibration of H_2O incorporation in cordierite and its application to high-grade metamorphism and crustal anatexis. *Journal of Petrology* **42**, 1595–620.

Harley, S. L. & Hensen, B. J. 1990. Archaean and Proterozoic high-grade terranes of east Antarctica (40–80°): a case study of diversity in granulite facies metamorphism. *In* Ashworth, J. R. & Brown, M. (eds) *High-temperature Metamorphism and Crustal Anatexis. Mineralogical Society Special Publication* **2**, 320–70.

Harley, S. L. & Motoyoshi, S. L. 2000. Al zoning in orthopyroxene in a sapphirine quartzite: evidence for >1120°C UHT metamorphism in the Napier Complex, Antarctica, and implications for the entropy of sapphirine. *Contributions to Mineralogy and Petrology* **138**, 293–307.

Hensen, B. J. 1971. Theoretical phase relations involving cordierite and garnet in the system $FeO\text{-}MgO\text{-}Al_2O_3\text{-}SiO_2$. *Contributions to Mineralogy and Petrology* **33**, 191–214.

Hensen, B. J. 1986. Theoretical phase relations involving garnet and cordierite revisited: the influence of oxygen fugacity on the stability of sapphirine and spinel in the system Mg-Fe-Al-Si-O. *Contributions to Mineralogy and Petrology* **92**, 362–7.

Hensen, B. J. & Green, D. H. 1973. Experimental study of the stability of cordierite and garnet in pelitic compositions at high pressures and temperatures. III. Synthesis of experimental data and geological applications. *Contributions to Mineralogy and Petrology* **38**, 151–66.

Holland, T. J. B., Babu, E. V. S. S. K. & Waters, D. J. 1996. Phase relations of osumilite and dehydration melting in pelitic rocks: a simple thermodynamic model in the KFMASH system. *Contributions to Mineralogy and Petrology* **124**, 383–94.

Holland, T. J. B. & Powell, R. 1990. An internally consistent thermodynamic dataset with uncertainties and correlations: the system $Na_2O\text{-}K_2O\text{-}CaO\text{-}MgO\text{-}MnO\text{-}FeO\text{-}Fe_2O_3\text{-}Al_2O_3\text{-}SiO_2\text{-}TiO_2\text{-}C\text{-}H_2\text{-}O_2$. *Journal of Metamorphic Geology,* **8**, 89–124.

Holland, T. J. B. & Powell, R. 1998. An internally consistent thermodynamic dataset for phases of petrological interest. *Journal of Metamorphic Geology* **16**, 309–43.

Hollis, J. & Harley, S. L. 2003. Alumina solubility in orthopyroxene coexisting with sapphirine and quartz. *Contributions to Mineralogy and Petrology* **144**, 473–83.

Holloway, J. R. & Blank, J. G. 1994. Application of experimental results to C-O-H species in natural melts. *In* Carroll, M. R. & Holloway, J. R. (eds) *Volatiles in Magmas. Mineralogical Society of America, Reviews in Mineralogy* **30**, 187–230.

Holtz, F. & Johannes, W. 1994. Maximum and minimum water contents of granitic melts: implications for chemical and physical properties of ascending magmas. *Lithos* **32**, 149–59.

Johannes, W. & Holtz, F. 1996. *Petrogenesis and experimental petrology of granitic rocks*. Berlin: Springer-Verlag.

Johannes, W. & Schreyer, W. 1981. Experimental introduction of CO_2 and H_2O into Mg-cordierite. *American Journal of Science* **281**, 299–317.

Kalt, A. 2000. Cordierite channel volatiles as evidence for dehydration melting: an example from high-temperature metapelites of the Bayerische Wald (Variscan Belt, Germasny). *European Journal of Mineralogy* **12**, 987–98.

Kelsey, D. E., White, R. W. & Powell, R. 2003. Orthopyroxene-sillimanite-quartz assemblages: distribution, petrology, quantitative P–T-X constraints and P–T paths. *Journal of Metamorphic Geology* **21**, 439–53.

Kriegsman, L. M. 2001. Partial melting, partial melt extraction and partial back reaction in anatectic migmatites. *Lithos* **56**, 75–96.

Kurepin, V. A. 1985. H_2O and CO_2 contents of cordierite as an indicator of thermodynamical conditions of formation. *Geochemistry International* **22**, 148–56.

Le Breton, N. & Schreyer, W. 1993. Experimental CO_2 incorporation in Mg-cordierite: non-linear behaviour of the system. *European Journal of Mineralogy* **5**, 427–38.

Markl, G., Bäuerle, J. & Grujic, D. 2000. Metamorphic evolution of Pan-African granulite facies metapelites from southern Madagascar. *Precambrian Research* **102**, 47–68.

Mirwald, P. W., Maresch, W. V. & Schreyer, W. 1979. Der Wassergehalt von Mg-cordierit zwischen 500° und 800°C sowie 0·5 und 11 kbar: *Fortschritte der Mineralogie* **57**, 101–2.

Mukhopadhyay, B. & Holdaway, M. J. 1994. Cordierite-garnet-sillimantie-quartz equilibrium I. New experimental calibration in the system $FeO\text{-}Al_2O_3\text{-}SiO_2\text{-}H_2O$ and certain $P\text{–}T\text{–}X_{H_2O}$ relations. *Contributions to Mineralogy and Petrology* **116**, 462–72.

Nandakumar, V. & Harley, S. L. 2000. A reappraisal of the pressure-temperature path of granulites from the Kerala Khondalite Belt, southern India. *Journal of Geology* **108**, 687–703.

Newton, R. C. & Wood, B. J. 1979. Thermodynamics of water in cordierite and some petrologic consequences of cordierite as a hydrous phase. *Contributions to Mineralogy and Petrology* **68**, 391–405.

Patiño Douce, A. E. & Johnston, A. D. 1991. Phase equilibria and melt productivity in the pelitic system: implications for the origin of peraluminous granitoids and aluminous granulites. *Contributions to Mineralogy and Petrology* **107**, 202–18.

Santosh, M. 1987. Cordierite gneisses of Southern Kerala, India: petrology, fluid inclusions and implications for crustal uplift history. *Contributions to Mineralogy and Petrology* **96**, 343–56.

Santosh, M., Jackson, D. H. & Harris, N. B. W. 1993. The significance of channel and fluid inclusion CO_2 in cordierite: evidence from carbon isotopes. *Journal of Petrology* **34**, 233–58.

Schenk, V. 1984. Petrology of felsic granulites, metapelites, metabasics, ultramafics, and metacarbonates from Southern Calabria (Italy): prograde metamorphism, uplift and cooling of a former lower crust. *Journal of Petrology* **25**, 255–98.

Schreyer, W. 1985. Experimental studies on cation substitutions and fluid incorporation in cordierite. *Bulletin de Minéralogie* **108**, 273–91.

Sheraton, J. W., Tingey, R. J., Black, L. P., Offe, L. A. & Ellis, D. J. 1987. Geology of Enderby Land and Western Kemp Land, Antarctica. *Bulletin Australian Bureau of Mineral Resources* **223**, 51 pp.

Skippen, G. B. & Gunter, A. E. 1996. The thermodynamic properties of H_2O in magnesian and iron cordierite. *Contributions to Mineralogy and Petrology* **124**, 82–9.

Stevens, G., Clemens, J. D. & Droop, G. T. R. 1995. Hydrous cordierite in granulites and crustal magma production. *Geology* **23**, 925–8.

Thompson, P., Harley, S. L. & Carrington, D. P. 2001. The distribution of $H_2O\text{-}CO_2$ between cordierite and granitic melt under fluid-saturated conditions at 5 kbar and 900°C. *Contributions to Mineralogy and Petrology* **142**, 107–18.

Thompson, P., Harley, S. L. & Carrington, D. P. 2002. Sodium and potassium in cordierite – a potential thermometer for melts? *European Journal of Mineralogy* **14**, 459–69.

Vielzeuf, D. & Holloway, J. R. 1988. Experimental determination of the fluid-absent melting relations in the pelitic system. Consequences for crustal differentiation. *Contributions to Mineralogy and Petrology* **98**, 257–76.

Vry, J. K., Brown, P. E. & Valley, J. W. 1990. Cordierite volatile content and the role of CO_2 in high-grade metamorphism. *American Mineralogist* **75**, 71–88.

Waters, D. J. 1988. Partial melting and the formation of granulite facies assemblages in Namaqualand, South Africa. *Journal of Metamorphic Geology* **6**, 387–404.

White, R. W., Powell, R. & Holland, T. J. B. 2001. Calculation of partial melting equilibria in the system $Na_2O\text{-}CaO\text{-}K_2O\text{-}FeO\text{-}MgO\text{-}Al_2O_3\text{-}SiO_2\text{-}H_2O$ (NCKFMASH). *Journal of Metamorphic Geology* **19**, 139–53.

White, R. W. & Powell, R. 2002. Melt loss and the preservation of granulite facies mineral assemblages. *Journal of Metamorphic Geology* **20**, 621–32.

Winkler, B., Milman, V. & Payne, M. C. 1994. Orientation, location, and total energy of hydration of channel H_2O in cordierite investigated by ab-initio total energy calculations. *American Mineralogist* **79**, 200–4.

SIMON L. HARLEY and P. THOMPSON, Grant Institute of Earth Science, School of GeoSciences, University of Edinburgh, Kings Buildings, West Mains Road, Edinburgh EH9 3JW, Scotland.
e-mail: sharley@glg.ed.ac.uk

MS received 17 October 2003. Accepted for publication 24 August 2004.